

# A Portable Heat Flux Sensor

P. Cousin, C. Gehin, J. Poujaud and N. Noury, *senior member, IEEE*

**Abstract**— Nowadays monitoring physiological signals in real situations is essential to get the best diagnosis on patients. In this study we focus on the heat flux generated by the human body. We are developing a portable heat flux sensor using specific thermal materials.

**Index terms**— heat flux, thermal sensor, wearable sensor.

## I. INTRODUCTION

Monitoring of physiological parameters in ambulatory situations [1] [2] is a challenge to meet the requirements of long term aftercare of patients in hospitals, or elderly people in home, but also for monitoring of athletes [3] during physical exercises.

Heat flux measurement is a particularly attractive physiological parameter as it is related both to metabolism and to the activation of autonomic nervous system.

There are already existing heat flux sensors, such as Gardon gauges, plug gauges and thin film thermocouple arrays [4] [5]. All of these sensors operate by measuring the temperature difference across a thermal resistance. We used a slightly different principle based on the thermal well allowing us a non-invasive implementation, more applicable for our needs.

The goal of this paper is to present our results concerning a flexible heat flux sensor, designed to be easily patched onto the skin in a non-obstructive manner, enabling long term monitoring in most of physical situations.

Different kind of thermal semiconductors associated with different insulators have been tested for the constitution of the sensor.

## II. MATERIAL AND METHODS

### A. Material

#### 1) Thermal canal

This experimentation is based on both thermal conduction and convection. Thermal conduction [6] is represented by the Fourier law (1).

$$\overrightarrow{\varphi(x)} = -\lambda \cdot \overrightarrow{\text{grad}(T)} = -\lambda \cdot \frac{\partial T}{\partial x} \quad (1)$$

$\varphi(x)$ : Heat flux ( $\text{W}\cdot\text{m}^{-2}$ )

$\lambda$ : Thermal conductivity ( $\text{W}\cdot\text{m}^{-1}\cdot\text{K}^{-1}$ )

T: Temperature (K)

x: Distance (m)

The law is really applicable with some restrictive hypothesis:

- To be in permanent regime
- The conductive body traversed by the heat flow is thermally insulated on the sides ( $\text{div } \varphi=0$ ).

On the other side, convection is the heat transfer from one place to another using at least one fluid. The combined process of thermal conduction and heat transfer is frequently called advection.

These two physical phenomena are involved in the experiment conducted here. For the later, we built a thermal canal which is composed by two materials of different thermal conductivities: a thermal semiconductor and a thermal insulator. The aim of this experimentation is to design the sensor with the best material for the flexible thermal canal arrangement.

For instance, copper is an excellent conductor with a thermal conductivity of  $390 \text{ W}\cdot\text{m}^{-1}\cdot\text{K}^{-1}$  and air, which is an excellent insulator, has a conductivity of  $0.0262 \text{ W}\cdot\text{m}^{-1}\cdot\text{K}^{-1}$ . Knowing that the human body has a thermal conductivity of  $0.5 \text{ W}\cdot\text{m}^{-1}\cdot\text{K}^{-1}$ , we thus selected semiconductor materials a close conductivity in order to not increase the inertia of the measure. Concerning insulator, we chose the expanded polystyrene which has thermal characteristics very similar to air. Moreover it is solid thus easier to give it the desired shape. In order to ensure flexibility, we can replace it by polyurethane with a lower thermal conductivity. In TABLE I. are presented thermal characteristics of the materials we experimented.

TABLE I. THERMAL CHARACTERISTICS OF SOME SYNTHETIC MATERIALS

Thermal materials		
Type of materials	Name	Conductivity ( $\text{W}\cdot\text{m}^{-1}\cdot\text{K}^{-1}$ )
Semiconductor	MED-2955	0.633
Semiconductor	MED-2980	1.56
Insulator	Expanded polystyrene	0.036

Pierre Cousin is with INL laboratory and Vigilio S.A. company, Innovation center, 5 avenue du Grand Sablon, 38700 La Tronche, France (pierre.cousin@insa-lyon.fr).

Claudine Gehin and Norbert Noury are with the INL laboratory in the Biomedical Sensors Group, site INSA, UMR 5270, Bâtiment Blaise Pascal, 7 avenue Jean Capelle 69621 Villeurbanne cedex, France (email: claudine.gehin@insa-lyon.fr, norbert.noury@insa-lyon.fr).

Julien Poujaud is with the Vigilio S.A. company, Innovation center (email: julien.poujaud@vigilio.fr).

Thermal materials		
Type of materials	Name	Conductivity ( $W.m^{-1}.K^{-1}$ )
Insulator	ABS plastic	0.17

The principle used in this experimentation is based on the thermal well [7]: when we place an insulator on top of a body generating heat, the thermal nets are modified. In this way a thermal well is produced which will pull up the deep body temperature to the body surface (Figure 1).

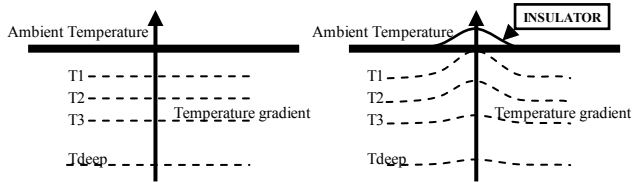


Figure 1. Thermal well.

It is necessary to impose a temperature gradient to determine the geometry of the canal. The gradient is set to 1 °C in order to measure variations in the range of 0.1 °C with a good accuracy. The section of the canal is a circle of 3 cm in diameter. Assuming an average metabolic heat production of 13000 kJ (150 W) [8] for the whole body, half of it (75 W) producing the heat flow at the skin interface, and considering an average skin surface of 1.8 square meters [9], we end with a thermal flow about 30 mW captured by our thermal canal (section 7 cm<sup>2</sup>), then the thermal resistance can be sized (2).

$$R_{th} = \frac{\Delta T}{\Phi} \quad (2)$$

R<sub>th</sub>: Thermal resistance (K.W<sup>-1</sup>)

ΔT: Temperature difference (K ou °C)

Φ: Heat flow (W)

According to (2), the thermal resistance can be determined (R<sub>th</sub> ≈ 34.3 K.W<sup>-1</sup>). Depending on the thermal conductivity of the materials we can determine the length of the canal (3).

$$R_{th} = \frac{1}{\lambda} \cdot \frac{L}{S} \quad (3)$$

λ: Thermal conductivity (W.m<sup>-1</sup>.K<sup>-1</sup>)

L: Length of the canal (m)

S: Area of the canal (m<sup>2</sup>)

TABLE II. CANAL LENGTH FOR THERMAL SEMICONDUCTOR

Thermal materials		
Type of materials	Name	Canal length (mm)
Semiconductor	MED-2955	15.2
Semiconductor	MED-2980	37.4

## 2) Physical thermal canals

Four configurations of thermal canals combining the 2 thermal semiconductors and the 2 thermal insulators (Figure 2) have been defined.



Figure 2. A thermal canal made with silicone thermal semiconductor (white core) insulated with polystyrene (blue envelop).

The four configurations were successively tested.

## 3) Experimental setup

For our experiments, a phantom reproducing a thermal gradient through a latex layer, mimicking thermal properties of the skin, was used (Figure 3). It consists in a heater, made with an aluminum plate in which circulates a heat transfer fluid (water). The whole is covered by a latex layer (thermal conductivity 0.4 W.m<sup>-1</sup>.K<sup>-1</sup>) imitating the skin. The fluid is driven with a peristaltic pump. The liquid temperature is monitored by a heating regulator activating a heating resistor. The temperature of this skin model ranges from 30 °C to 43 °C which mimics the skin temperature range.



Figure 3. Physical model of skin.

The top surface of the skin model was characterized to determine the thermal uniformity using a thermal infrared camera (FLIR i50, FLIR, USA).

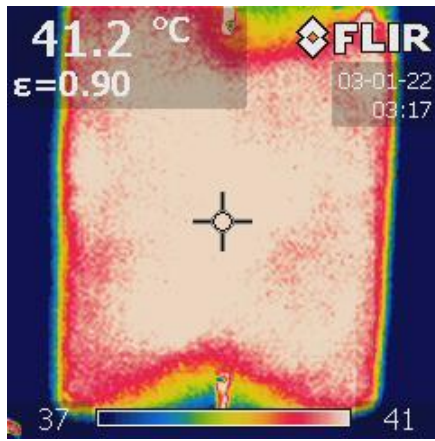


Figure 4. Thermal imaging of the skin model.

As the model was not uniform (Figure 4), we decided to fully characterize only one point of the skin. Two thermistors were placed on top and under the latex layer in order to figure differences in temperature observed, for several temperatures of control. Thus a calibration curve of our model can be determined (Figure 5).

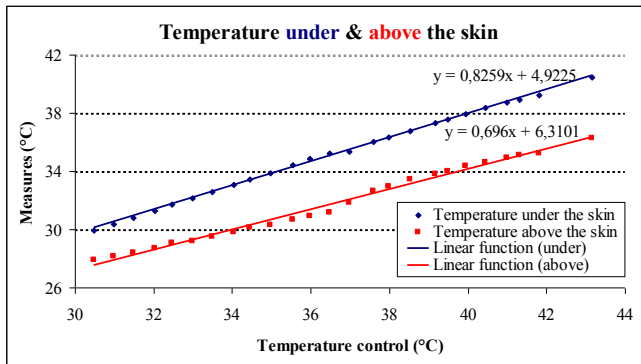


Figure 5. Calibration curve of the model.

The calibration curve shows that  $\Delta T$  between temperatures under and over the skin tends to increase with the temperature. Between the first point of measurement (30.5 °C) and the last one (43.16 °C),  $\Delta T$  increases from 2.06 °C to 4.02 °C. This is due to the heating of materials which becomes more conductive with the increasing number of thermal phonons in the material.

#### 4) Instrumentation

All temperatures were measured with Negative Temperature Coefficient Thermistors (CTN 10 K $\Omega$ , MA100GG103A, GE SENSING) which feature an accuracy of 0.1 °C and a sensibility of 0.01 °C. Each thermistor channel was connected to a Wheatstone bridge with precision resistors 10 K $\Omega$ .

Data acquisition of signals was performed with the PowerLab 26T (ADInstruments, Cambridge) coupled to resistors bridges. We used the 4 channels, one dedicated to the reference temperature (water), one for the temperature

under the "skin" of the model, one for the "South" of the canal (close to skin) and one for the "North" (far from the skin). The conversion in °C was made with the LabChart Pro Software provided with PowerLab 26T. The three thermistors (under the skin and the two of the canal) were aligned on a same vertical axe.

Even if the phantom was insulated from external environment by a plastic box to prevent from air movement, the temperature inside the box increased during the experimentation so we decided to monitor also the inbox temperature

#### B. Methods

To configure the phantom, the operating speed of the pump was set to 390 ml.min<sup>-1</sup> during our different tests. Each thermistor was calibrated and possible correction was taken into account when acquiring with PowerLab 26T.

The experimental protocol consisted in applying incremental steps of 1°C at each new point and wait for stabilization thereof. The phantom exhibits a large inertia, and thus a long stabilization time (dozens of minutes).

Eventually, we characterized the step response and the static temperature differences between the measuring points.

### III. RESULTS

Concerning static data, we have carefully studied the behavior of different materials as well as changes in ambient temperature. We notice that polystyrene is a better insulator than ABS, as it was expected regarding their characteristics (Table I). Indeed, the  $\Delta T$  between the two extremities of the canal is closer to the 1 °C that we set (Figure 6 & Figure 7).

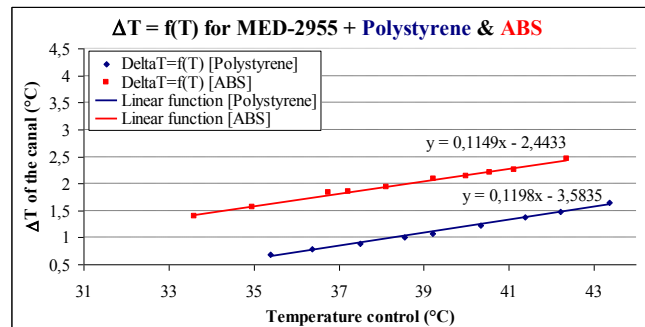
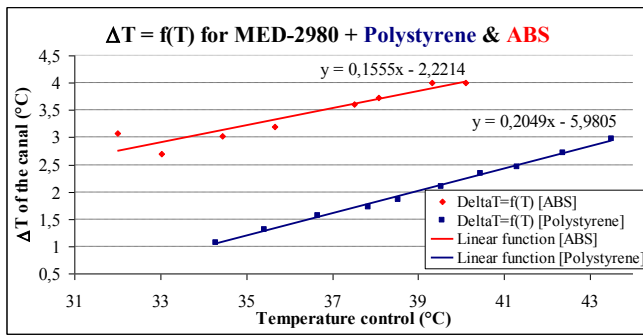
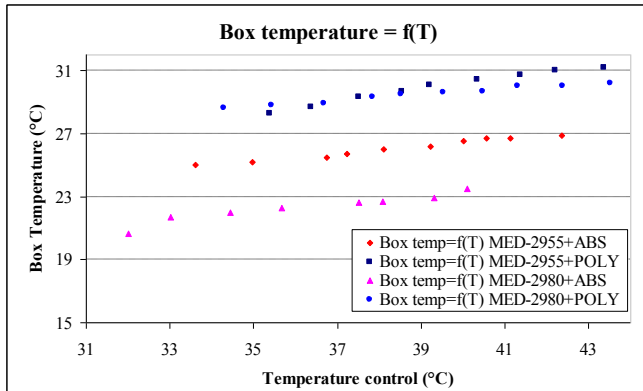


Figure 6. Characterization of MED-2955 for ABS (red line) and for polystyrene insulators (blue line).



**Figure 7. Characterization of MED-2980 for ABS (red line) and for polystyrene insulators (blue line).**

The MED-2955 offers better results than for the MED-2980: the variation around the gradient of 1 °C is lower as well as the temperature gradient between ABS and polystyrene.



**Figure 8. Temperature variations inside the box.**

Moreover, we notice that the  $\Delta T$  of the canal increases with the temperature control (Figure 8). This is mainly due to the heating of materials which is partly caused by the increase in temperature of the set point and also the increase in temperature inside the plastic box. Note that for all configurations of thermal canal the temperature in the box increases of around 2.3 °C.

#### IV. DISCUSSION AND CONCLUSION

Following our experiments, we can conclude that a thermal canal made of thermal semiconductor MED-2955 in association with a polystyrene insulator, makes a reliable and precise thermal canal. The MED-2955, with a thermal conductivity (i.e.  $0.633 \text{ W}\cdot\text{m}^{-1}\cdot\text{K}^{-1}$ ) close to the human body allows the canal to maintain the temperature gradient in the range of the 1 °C gradient as we set from the beginning. Concerning the polystyrene, which is a good insulator and easier to cut material, it reduces the error between the temperature control and the measure.

However the trials show that the model has a high inertia (20 to 30 minutes are needed to stabilization of the

measures). Thanks to a dynamic analysis of the data and by identifying the mathematical model for a step response, we expect to be able to precisely determine the final value based on the first samples of the dynamic response. We already identified a model that is a product of 1<sup>st</sup> orders and the validation of this model is ongoing on the data collected.

As we now control the process to measure heat flux, further work will focus on the miniaturization of electronics and reduction of material thicknesses in order our sensor to be easily integrated in embedded applications.

The thickness will be particularly prohibitive when the sensor will be patched on the skin of the subject.

#### REFERENCES

- [1] E.T. McAdams, C. Gehin, N. Noury, C. Ramon, R. Nocua, B. Massot, A. Oliveira, A. Dittmar, C.D. Nugent and J. McLaughlin, "Biomedical Sensors for Ambient Assisted Living", in *Advances in Biomedical Sensing, Measurements, Instrumentation and Systems*, Lecture Notes in Electrical Engineering, (2010), Vol. 55, 240-262.
- [2] E. Campo, D. Hewson, C. Gehin, N. Noury, "Theme D: Sensors, wearable devices, intelligent networks and smart homecare for health", IRBM, Volume 34, Issue 1, February 2013, pp. 11–13.
- [3] A. Sabo, P. Kafka, S. Litzenberger, C. Sabo, "Physiological monitoring system for high altitude sports"
- [4] R. Gardon, "An Instrument for the Direct Measurement of Intense Thermal Radiation, Review of Scientific Measurements", 24, 5, 1953, pp. 366-370.
- [5] H. Will, "Fabrication of Thin Film Heat Flux Sensors", Proceedings of the Third Health Monitoring Conference for Space Propulsion Systems, 1991, Cincinnati, OH, pp.348-355.
- [6] R.W. Serth, T.G. Lestina, "1 - Heat conduction", in *Process Heat Transfer (2nd Edition)*, 2014, pp. 1-30.
- [7] R.H. Fox, A.J. Solman, "A new technique for monitoring the deep body temperature in man from the intact skin surface", Proceedings of the physiological society, 1970.
- [8] Harris JA, Benedict FG. A biometric study of basal metabolism in man, Washington, DC: Carnegie Institute of Washington; 1919 Publ. n°279.
- [9] Mosteller RD. Simplified calculation of body-surface area. *N Engl J Med* 1987;317:1098.